Single-Epoch Integer Ambiguity Resolution with GPS-GLONASS L1-L2 Data

M. Pratt, B. Burke, and P. Misra
Lincoln Laboratory, Massachusetts Institute of Technology

Abstract: The effectiveness of single-epoch integer ambiguity resolution, which provides centimeter-level relative positioning in real-time, is a function of the number, quality and type of carrier phase measurements available**.** We apply the Local-Minima Search (LMS) method epoch-by-epoch to GPS-GLONASS dual frequency carrier phase measurements taken over 2, 9 and 18 km baselines. While the application of LMS to GPS dual frequency measurements alone works quite well over these baselines, the addition of GLONASS improves the search success rate and greatly enhances the ability to validate the resulting solutions. At both 9 km and 18 km the LMS success rate was nearly 100%, when using the combined set of carrier phases. The addition of GLONASS reduced the average search ratio by more than 1/3 over the ratio obtained using only GPS phases. A fuller GLONASS constellation will certainly improve on these results.

I. INTRODUCTION

The ability to resolve carrier phase ambiguities using just the measurements from a single epoch has several important benefits. First, such methods are immune to corruption from cycle slips, and secondly, they provide centimeter-level relative positioning immediately. However, single-epoch methods, as they exist today, are not reliable enough for many common applications, such as aircraft precision approach. There are 2 major ways to improve reliability. One is to add more measurements, the other is to reduce the errors in the measurements. In [1] we demonstrated that it was possible to effectively reduce measurement errors by using multiple reference stations. In this paper, we demonstrate the incremental benefit provided by adding more measurements, in this case in the form of dual-frequency GLONASS carrier phases.

The addition of GLONASS measurements introduces the complication of multiple frequencies, since GLONASS is a Frequency Division Multiple Access (FDMA) system. In [2], we showed that GLONASS L1 carrier phases could be included without altering the structure of the integer ambiguity problem. In this paper, we show that those arguments are strengthened by the availability of GLONASS L2 phases. Although GLONASS does not complicate the integer problem, it does require that the receiver and antenna be calibrated for frequency-dependent delays. If such delays exist they must be stable with respect to expected temperature variations, or the measurements may have unacceptable biases. The data we collected showed consistent - and therefore removable – frequency-dependent delays.

Several methods [1-6] have been proposed for single-epoch ambiguity resolution. In this paper we use a slightly modified form of the Local-Minima Search (LMS) method [1,2]. LMS finds the subset of potential integer solutions that are local minima of an unweighted least-squares cost function. This subset, which is of manageable size, is then reevaluated with a weighted cost function. It was found that there are epochs at which the correct integers are local minima of the unweighted cost function, but are not the global minimum. The separation of the problem into two steps shows promise as the second cost function evaluation can use information, such as baseline length, to help judge potential integer solutions.

The measurements and results discussed in this paper were obtained with a pair of Ashtech Z-18 receivers with prototype helix antennas. Ashtech Z-18 receivers can track up to 10 GPS and 8 GLONASS satellites, and provide code and carrier measurements at both L1 and L2 for each satellite. This new product was announced only recently, and our work is in a sense a beta test for the receivers. Unfortunately, the GLONASS constellation is down to 13-14 working satellites, and we had to schedule data collection to take advantage of periods during which 3-4 GLONASS satellites would be in view. The scarcity of GLONASS satellites was somewhat offset by the more-than-full GPS constellation of 27 satellites.

The paper is organized as follows: In section II, we formulate the basic double-difference equations for

ION GPS-98

GLONASS carrier phase measurements and discuss the role that GLONASS frequency structure plays in double-differences. We show that the FDMA structure of GLONASS causes some double difference equations to be more accurate than others, and so affects our choice of which integers to work with. Section III covers receiver and antenna calibration and some receiver problems we encountered. We also briefly mention GPS-GLONASS double differences. In Section IV we present results for three data sets and use these results to demonstrate the incremental benefit of GLONASS carrier phase measurements.

II. GPS-GLONASS DUAL FREQUENCY DOUBLE DIFFERENCES

The fundamental carrier phase double-difference equation for satellites *i* and *j* applicable to both GPS and GLONASS can be written as,

$$\varphi_\beta^{ij} = k_\beta^i r^i - k_\beta^j r^j + (k_\beta^i - k_\beta^j)b + N_\beta^{ij} + A_\beta^{ij} \qquad (1)$$

The subscript β indicates the frequency band, 1 or 2. In (1), the following apply,

$$A_\beta^{ij} = k_\beta^i T^i - k_\beta^j T^j - \left(k_\beta^i \frac{I^i}{(f_\beta^i)^2} - k_\beta^j \frac{I^j}{(f_\beta^j)^2} \right) \qquad (2)$$

φ_β^{ij}	L_β double difference carrier phase
r^i	range single difference
k_β^i	L_β wave number (f_β^i / C).
b	single difference of receiver clock bias.
N_β^{ij}	double-difference integer ambiguity.
T^i	single difference of tropospheric delay
I^i	single difference of ionospheric advance
f_β^i	L_β carrier frequency

For GPS the wave numbers k_β^i are independent of the

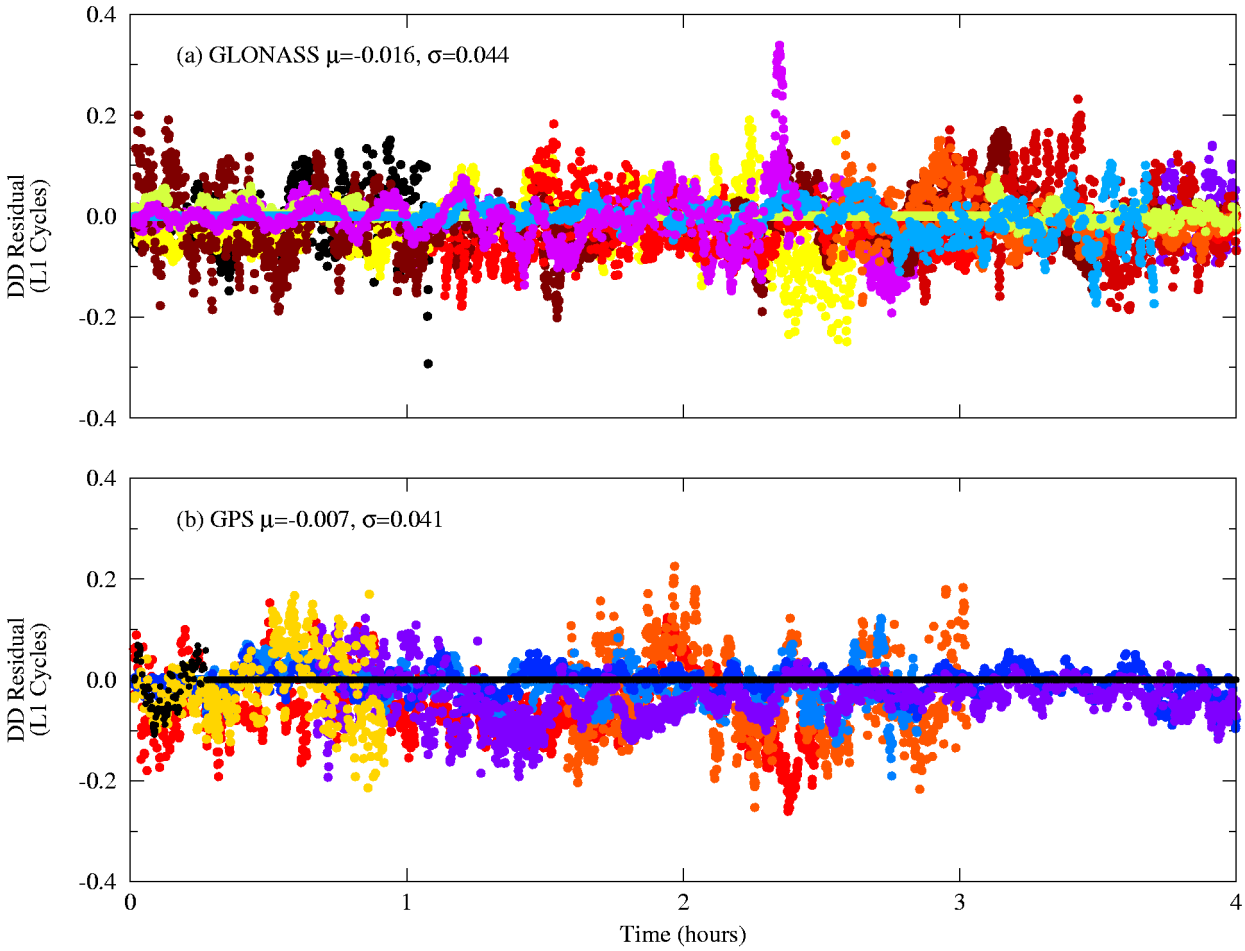

Figure 1: *Effect of receiver clock bias error on GLONASS double differences.*

satellite index *i* and, therefore the clock bias term drops out in equation (1). For GLONASS, the wave numbers are given by [7],

$$k_\beta^i = c_\beta (178 + \frac{i}{16}) \quad \text{(cycles/m, i=1,2,…,23)} \qquad (3)$$

In equation (3) above, c_β is 9 for L1 (β=1), 7 for L2 (β=2), and 2 for wide-lane (β=w). As a result, the clock bias coefficient in (1) is

$$k_\beta^i - k_\beta^j = (i-j)\frac{c_\beta}{16} \qquad (4)$$

As presented in [2], we handle the clock bias term in GLONASS double differences by using an estimate for b based on differential pseudoranges. The error committed will be the coefficient (4) times the error in the estimate for b. We argued previously that this error is negligible for L1 double differences. For L2 and wide-lane double differences, the error is even smaller by a factor of 7/9 and 2/9 respectively, and this fact plays a role in our selection of integers. Figure 1 shows L1 double-difference residuals as a function of time for both GLONASS and GPS. The data was collected with a 2-km baseline and so has typical clock estimate errors. The standard deviations are 0.044 for GLONASS and 0.041 for GPS, both in L1 cycles. This represents an acceptable increase in measurement error.

According to [7], stage 2 of the plan to shift GLONASS frequencies will limit the frequency indices *i* and *j* in (4) to the range 1,2,…,12. This shift, expected to take place in the 1998-2005 time frame, will further reduce the magnitude of the clock error in the double differences. A final point about the clock error: it might be expected that the availability of GLONASS pseudoranges would improve the accuracy of the clock bias estimate.

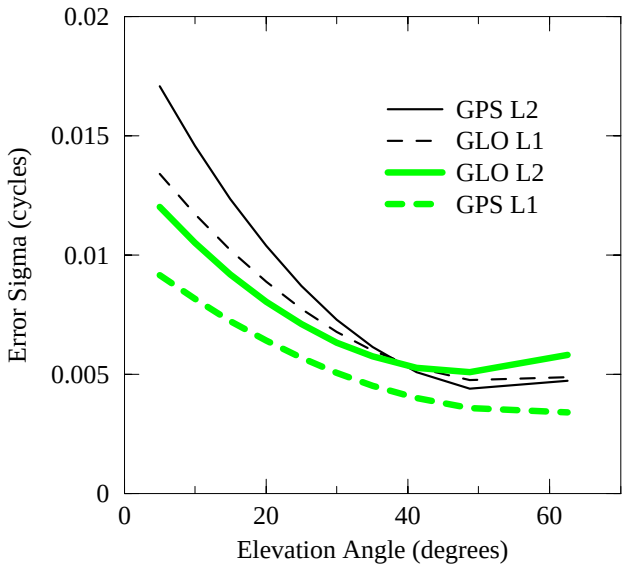

Figure 2: *Double difference measurement quality as a function of elevation angle.*

This was not the case, however, as the Z-18 GLONASS pseudoranges had significant frequency-dependent biases.

Wide-lane is the difference of L1 and L2 phases, and so wide-lane, L1 and L2 integers form a linearly dependent set, from which an independent subset is chosen. The choice of which double-difference integers to include in the search is made by selecting those with the least expected measurement error as expressed in cycles. Because tropospheric effects are perfectly correlated on L1 and L2, their effect on wide-lane measurements is scaled down by an amount equal to the increase in wavelength. The situation with ionospheric effects is similar but not quite as good since the dependence of ionospheric advance on frequency degrades the L1-L2 correlation. The upshot is that wide-lane measurements have smaller atmospheric errors (in cycles) than either L1 or L2 and so wide-lane integers are the first choice for ambiguity resolution. Unfortunately, there are not enough wide-lane integers for a reliable search, and they must be augmented with L1 and/or L2 integers. To decide which other double-difference integers to include, RMS values of zero-baseline residuals were plotted as a function of elevation angle as shown in Figure 2. For GPS, L2 is encrypted, and the resulting loss in SNR gives noisier measurements, as shown. It follows that for GPS we use L1 integers to go along with wide-lane integers. For GLONASS, L2 is not encrypted, and it can be seen that the GLONASS L2 double differences are in fact slightly better than the L1 differences. This has two benefits: L2 is a longer wave than L1, and the clock bias errors for L2 double differences are smaller that for L1 since c_β is 7 for L2 and 9 for L1.

III. MEASUREMENT CALIBRATION

If the receiver or the antenna produces signal delays that depend on frequency, then these delays will show up as biases in the double-differenced phase measurements [8]. In Figure 3, zero-baseline double-difference residuals are plotted as a function of the frequency difference of the satellites involved. The L1 residuals in the upper panel (a) clearly show a linear bias. The lower panel (b), corresponding to L2, is unbiased. Using the frequency difference as the independent variable gives a clear picture only if the delays are a linear function of frequency. Fortunately, that appears to be the case.

Zero-baseline data tells you nothing about delays caused by mismatched antennas. To calibrate the antennas, the procedure described above is repeated using very short-baseline data. We found that the antennas caused additional linear delays at L1, but not at L2. The existence of frequency dependent delays for the Z-18 surprised us since we have considerable experience with

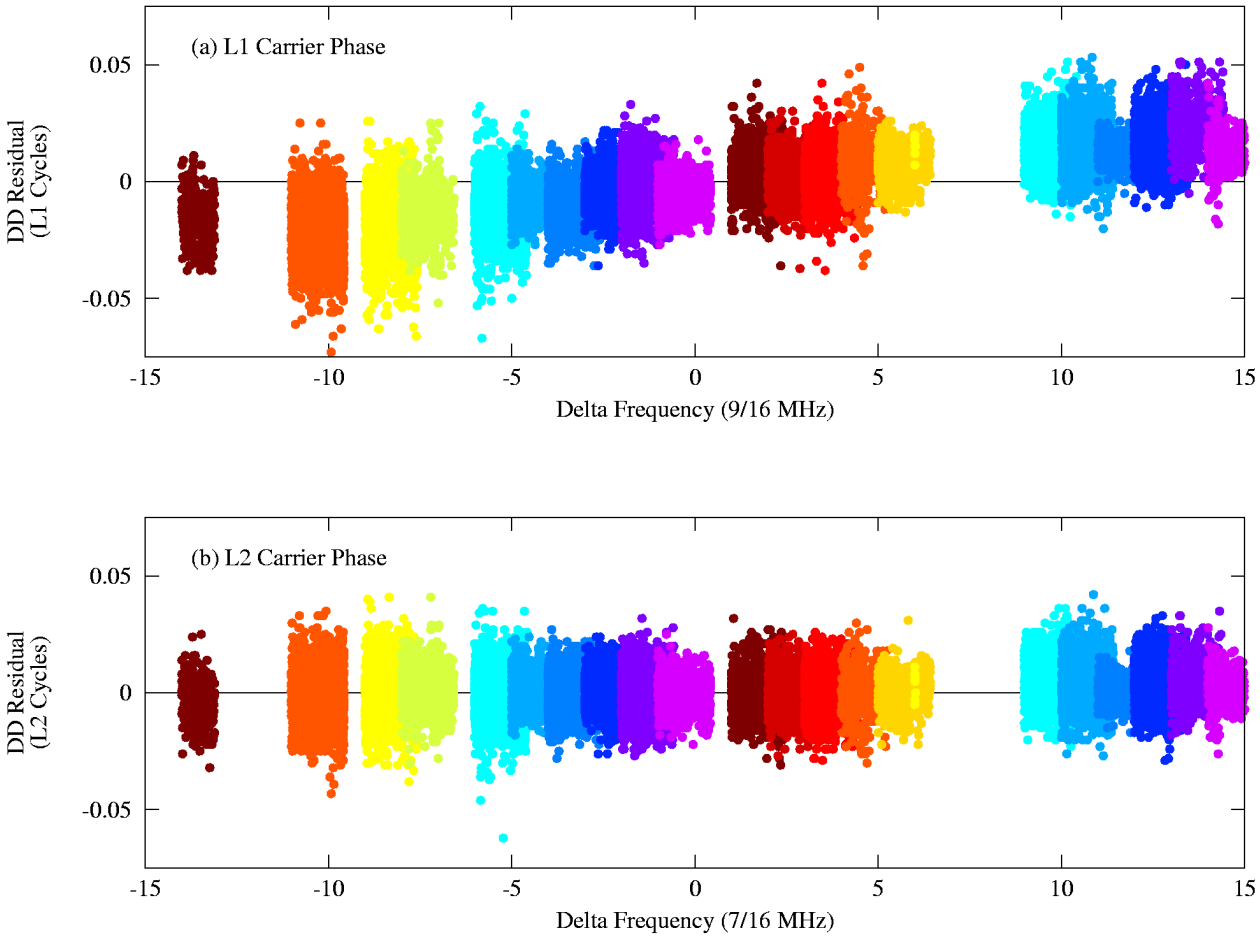

Figure 3: *GLONASS carrier phase calibration.*

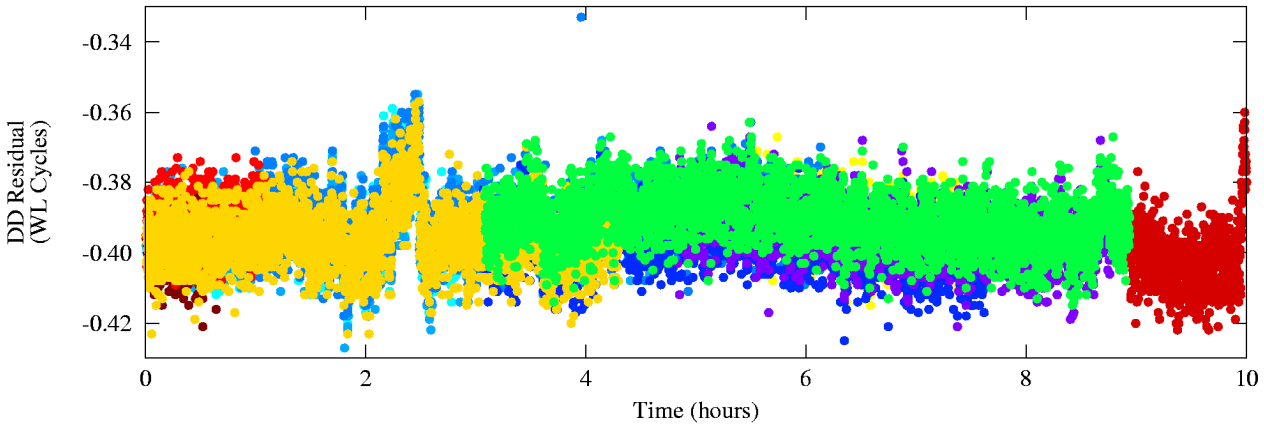

Figure 4: GPS-*GLONASS carrier phase calibration.*

Ashtech GG-24s, and we haven't seen calibration problems with GG-24 carrier phases.

Until this point, no mention has been made of forming GPS-GLONASS double differences. This is an attractive idea because it results in additional independent integer unknowns, and ambiguity resolution improves as more integers are added. There are two potential problems with GPS-GLONASS double differences. First, if the frequencies are too far apart, then the receiver clock bias error will be too large, and second, there can be calibration type biases. Since the frequency of GPS wide-lane is 347.82 MHz, and of GLONASS 356+*i*/8 MHz, the difference is approximately 10 MHz. A 10 MHz frequency difference is small enough that clock errors should be acceptable. The same can't be said for L1 or L2 differences since the in these cases the GPS-GLONASS frequency deltas are approximately 20 and 30 MHz respectively. Restricting attention to wide-lane, Figure 4 shows residuals resulting from differencing each GLONASS first difference with the first difference of the highest elevation GPS satellite for a 10-hour period in a zero-baseline test. As can be seen, these residuals are biased, and the bias is essentially constant. If all data sets demonstrated the same GPS-GLONASS bias, then it could have been removed. Unfortunately, each of our data sets showed a different bias. For this reason, GPS-GLONASS double differences were not used in this study.

Two measurement problems other than calibration were encountered. Two of the data sets had unexplained constant biases between GLONASS L1 measurements. No bias was seen in the L2 measurements. These biases were removed via postprocessing. The second problem is harder to describe. It manifested itself as a large and rapidly changing error in the L1 measurement of a few GPS phases. The measurements for almost the entire satellite track appeared normal, and then as the satellite set the phase measurement showed large and rapidly changing errors. These errors were not consistent with atmopheric effects or multipath. Again, these problems were identified during postprocessing and eliminated.

IV. RESULTS

Data were collected with baselines of 2 km, 9 km and 18 km using a 5-second interval. The data were processed using the LMS algorithm epoch by epoch to resolve GPS L1, GLONASS L2 and wide-lane integers. The results are summarized in the table below. A position estimate with an error of less than 10 cm is considered successful.

Figure 5 presents data and results for measurements from the 2-km baseline for a 3-hour period. The four panels are as follows: Panels (a) and (b) show double-difference ionospheric errors and unmodeled tropospheric errors respectively, each in L1 cycles. The equations for these are given in the Appendix. The troposphere was modeled using UNB4, a model developed at the University of New Brunswick [9]. Panel (c) shows wide-lane residuals, in wide-lane cycles. In Panels (a), (b), and (c), different gray levels identify satellites. Panel (d) shows the search ratio resulting from two runs of LMS: black corresponding to the use of GPS measurements only, gray the combination of GPS and GLONASS. The search ratio is the ratio of the smallest cost function value to the second smallest and is a measure of our confidence in the solution. A smaller ratio implies more confidence.

Baseline	Time Span h:mm	Number of Samples	GPS Only No. Successful (% of total)	GPS+GLO No. Successful (% of total)
2 km	4:00	2880	2873 (99.76%)	2875 (99.83%)
9 km	2:10	1565	1563 (99.87%)	1565 (100%)
18 km	1:55	1381	1354 (98.05%)	1380 (99.93%)

For the 2-km data, both the GPS only and the GPS+GLONASS runs settled on the correct integers almost 100% of the time. There were a few epochs near the end of the data set that had large measurement errors on one GPS satellite, perhaps due to interference or a receiver failure. These points, seen in Figure 5 as having unreasonable ionospheric and tropospheric estimates and large wide-lane residuals caused all of the failures. Even though the performance of the two runs was similar, the resulting search ratios were significantly different. The average ratio for the GPS only run was 0.16, for the combined run the average was more than 1/3 less, or 0.1. If a ratio of ½ is used as a validation threshold, then the GPS-only case would have 63 false alarms and 1 missed detection. On the other hand, the combined GPS+GLONASS run would have 11 false alarms and no missed detection.

One final note on Figure 5. These measurements are extremely noisy, there appears to be significant multipath relative to the figures that follow. This data set was collected on a rooftop using an antenna with no choke ring, in proximity to many potential reflection sources.

The 9-km and 18-km results are shown in Figure 6 and 7 respectively. Each of these figures presents the same information as was given in Figure 5. At 9-km, Figure 6, the GPS-only search found the correct integers 99.87% of the time (2 failures), the GPS+GLONASS 100%. Vertical lines in panel (d) identify the epochs at which the GPS only search failed. Once again, the addition of GLONASS measurements reduced the average search ratio by about 30%, going from 0.15 to 0.1. A validation threshold of ½ would result in 58 false alarms with no missed detection for GPS only, and 3 false alarms

and no missed detection for GPS+GLONASS. Panel (b) of Figure 6 shows tropospheric effects emerging from the multipath, although panel (a) still doesn't show any identifiable ionospheric effects. Even with the significant (0.4 cycle) residual unmodeled tropospheric delay in panel (b), the wide-lane residuals are very small. This effect will be seen even more clearly in Figure 7. Since ambiguity resolution is essentially a measurement consistency check, it follows that using only wide-lane measurements should enhance the search success rate, and this is one of the real promises of GLONASS. When a full constellation is deployed, there may then be enough wide-lane measurements to make wide-lane only searches reliable.

The 18-km baseline data, shown in Figure 7, resulted in success rates of 98.05% and 99.93% for the GPS only and GPS+GLONASS cases respectively. The average search ratio improved from 0.19 to 0.13. Panel (a) shows some ionospheric errors (0.25 cycles) and large tropospheric errors (0.75 cycles). The wide-lane residuals in panel (c) are still quite small with an RMS value of 0.046

One final comment about Figures 5-7. The correct metric for evaluating the performance of a search method is the magnitude of measurement errors that can be successfully dealt with, and not the baseline length. This was the reason for including the ionospheric advance and unmodeled tropospheric delay panels in these figures. To be complete, a measure of multipath error is also needed.

V. SUMMARY

We have demonstrated that augmenting GPS dual-frequency carrier phase measurements with those from GLONASS improves both the performance and integrity of single-epoch ambiguity resolution. The addition of GLONASS L2 carrier phases both improves the quality of double differences available and holds out the promise of wide-lane only solutions. Calibration issues, while a concern, were found to be manageable.

The data sets used for this study were collected over only 2-4 hours. In order to claim success for an algorithm over a certain baseline, measurements would be required for much longer periods, perhaps over weeks and months, in order to experience typical atmospheric variations.

ACKNOWLEDGMENTS

We thank Magellan Corp. and, in particular, Dr. Frank van Diggelen for timely support with Ashtech Z-18s. This work was sponsored by the Federal Aviation Administration under research grant 97-G-010. The authors are grateful to Ray Swider, FAA LAAS program manager for his support. The opinions, interpretations, conclusions and recommendations presented in this paper are those of the authors, and are not necessarily endorsed by the FAA.

REFERENCES

[1] M. Pratt et al., "Single-Epoch Integer Ambiguity Resolution with GPS L1-L2 Carrier Phase Measurements," *Proc. ION '97*, The Institute of Navigation, pp. 1737-1746, 1997.

[2] M. Pratt et al., "Single-Epoch Integer Ambiguity Resolution with GPS-GLONASS L1 Data," *Proc. ION 53rd Annual Meeting*, The Institute of Navigation, pp. 691-699, 1997.

[3] S. Han and C. Rizos, "Integrated Method for Instantaneous Ambiguity Resolution Using New Generation GPS Receivers," *IEEE PLANS '96*, pp. 254-261, 1996.

[4] S. Han, "Quality Control Issues Relating to Instantaneous Ambiguity Resolution for Real-Time GPS Kinematic Positioning," *Proc. ION GPS-96*, The Institute of Navigation, pp. 1419-1430, 1996

[5] S. Han, "An Instantaneous Ambiguity Resolution Technique for Medium-Range GPS Kinematic Positioning," *Proc. ION GPS-97*, The Institute of Navigation, pp. 1789-1800, 1997

[6] R. Hatch, "Instantaneous Ambiguity Resolution," *Proc. Kinematic Systems in Geodesy, Surveying, and Remote Sensing*, KIS Symposium, Banff, Canada, pp. 299-308, 1990.

[7] GLONASS Interface Control Document, Moscow, 1995.

[8] S. Gourevitch et al, Ashtech RTZ Real-Time Kinematic GPS with OTF Initialization, " *Proc. ION GPS-95*, The Institute of Navigation, pp. 167-170, 1995.

[9] P. Collins et al., "Limiting Factors in Tropospheric Propagation Delay Error Modeling for GPS Airborne Navigation," *Proc. ION 52nd Annual Meeting*, The Institute of Navigation, pp. 519-528, 1996.

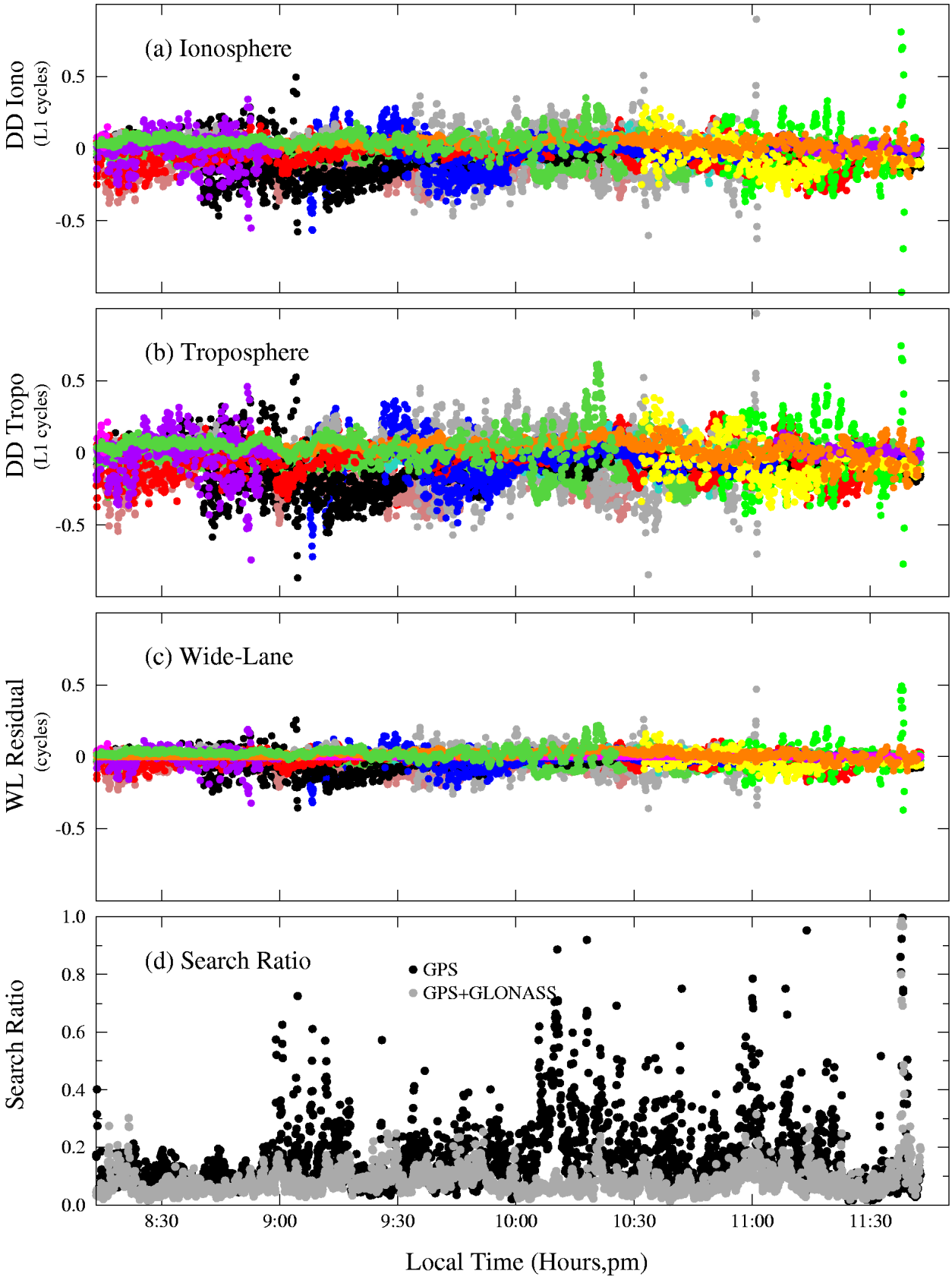

Figure 5: *2-km baseline DD measurement errors and single-epoch integer search ratio.*

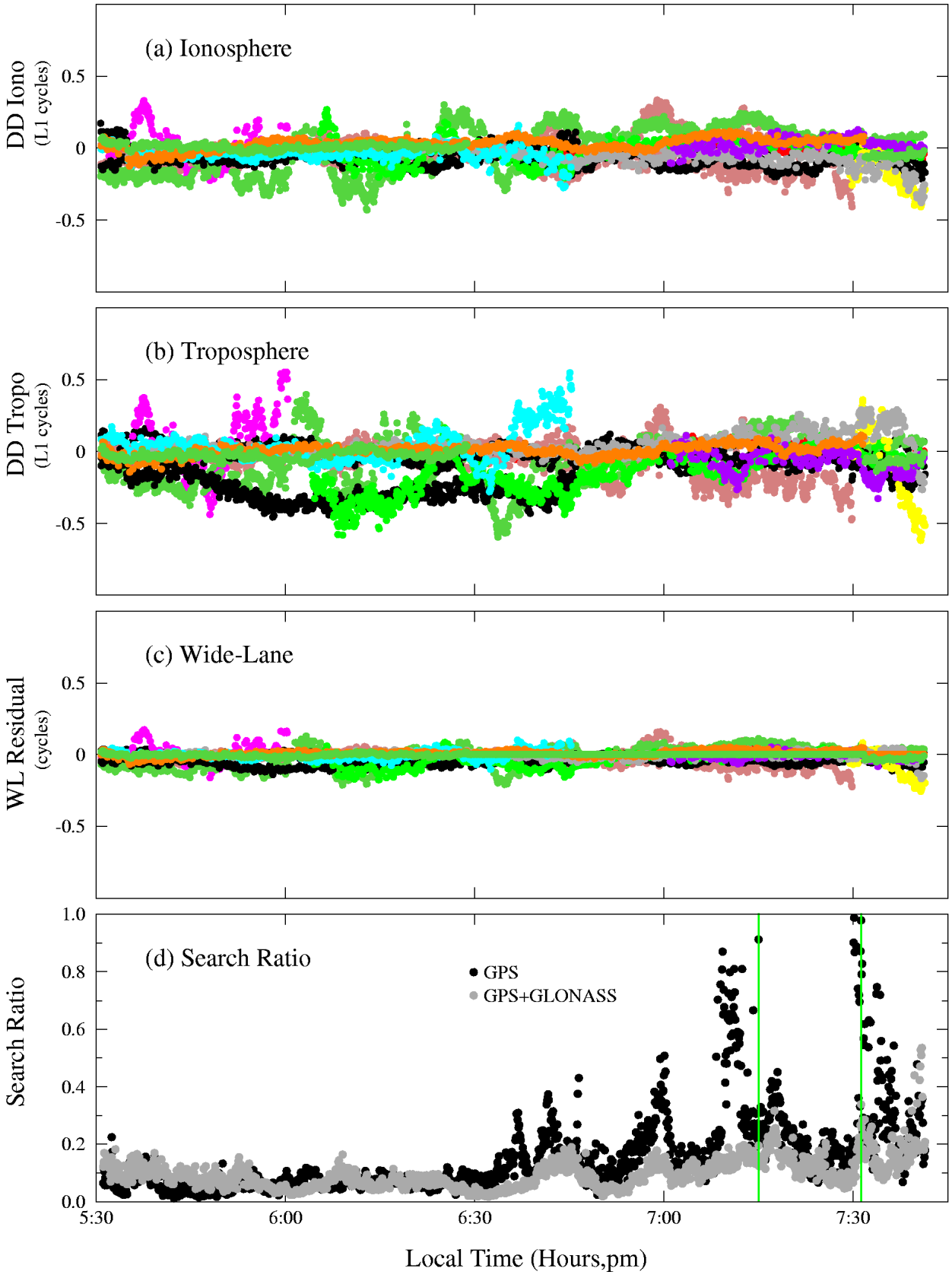

Figure 6: *9-km baseline DD measurement errors and single-epoch integer search ratio.*

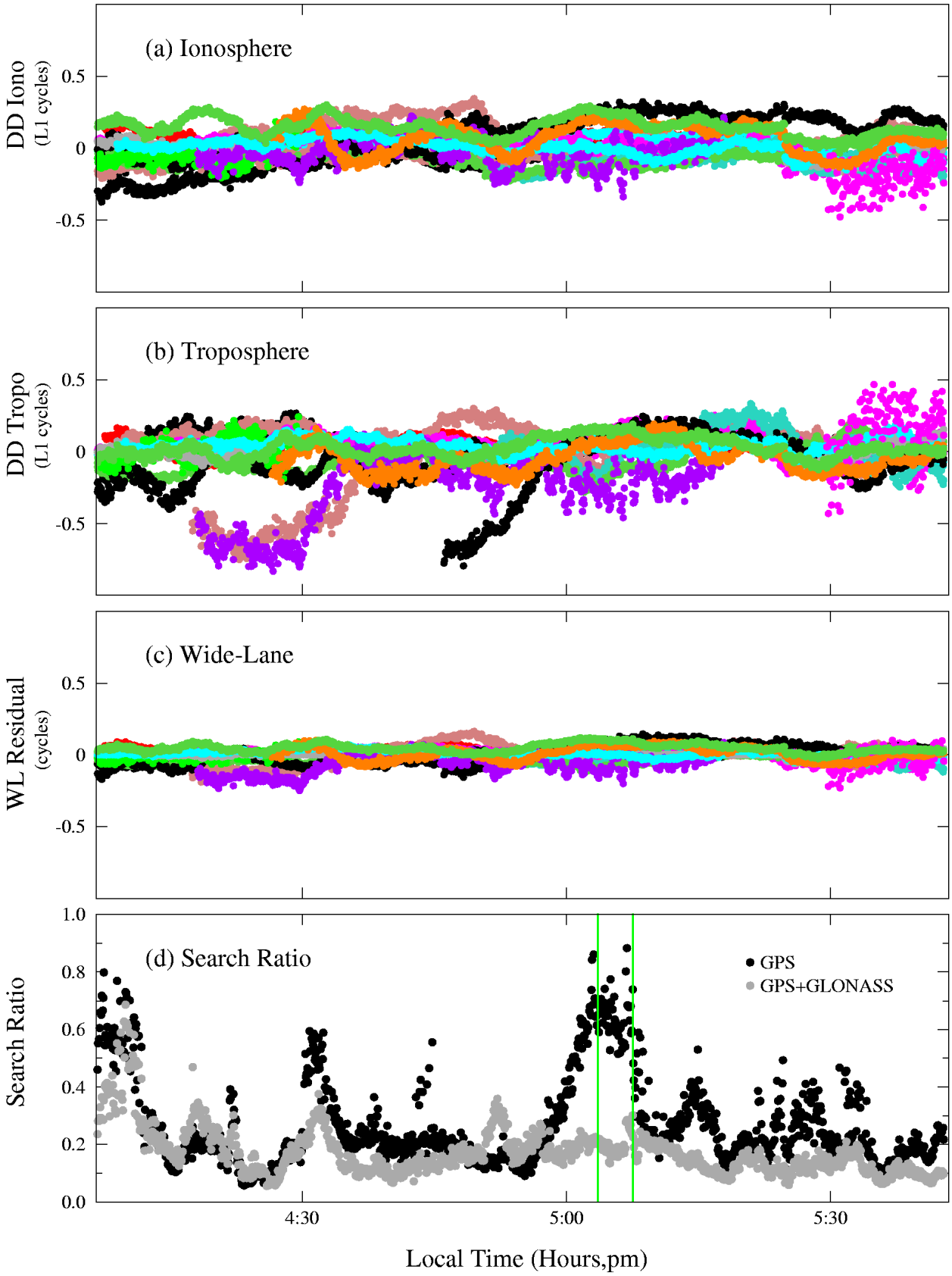

Figure 7: *18-km baseline DD measurement errors and single-epoch integer search ratio.*

APPENDIX. Derivation of GLONASS Ionospheric and Tropospheric Terms

As is well known, GPS dual frequency measurements can be used to form the ionosphere-free and the geometry-free (ionospheric estimate) combinations. We now show that the same is true for GLONASS. First some notation. Let $I_{1i}^i = I^i / \left(f_1^i\right)^2$ be the ionospheric advance for satellite *i* in meters at the *i*-th L1 frequency (L_1^i). At L2 the *i*-th satellite ionospheric advance is scaled to meters at L_1^i as follows,

$$\frac{I^i}{\left(f_2^i\right)^2} = \left(\frac{f_1^i}{f_2^i}\right)^2 \frac{I^i}{\left(f_1^i\right)^2} = \left(\frac{f_1^i}{f_2^i}\right)^2 I_{1i}^i$$

We now simplify this expression using the following relationship,

$$\frac{f_1^i}{f_2^i} = \frac{k_1^i}{k_2^i} = \frac{9 \cdot (178 + i/16)}{7 \cdot (178 + i/16)} = \frac{9}{7}$$

Since this ratio is independent of *i,* we will write k_1^i / k_2^i as k_1 / k_2, from which it follows that $k_2^i = (k_2 / k_1) k_1^i$. Using the above, the GLONASS L1 and L2 double-difference phase equations are:

$$\varphi_1^{ij} = k_1^i r^i - k_1^j r^j + (k_1^i - k_1^j) b + N_1^{ij} + k_1^i T^i - k_1^j T^j - k_1^i I_{1i}^i + k_1^j I_{1j}^j$$

$$\varphi_2^{ij} = \tfrac{k_2}{k_1}(k_1^i r^i - k_1^j r^j) + \tfrac{k_2}{k_1}(k_1^i - k_1^j) b + N_2^{ij} + \tfrac{k_2}{k_1}(k_1^i T^i - k_1^j T^j) - \tfrac{k_1}{k_2} k_1^i I_{1i}^i + \tfrac{k_1}{k_2} k_1^j I_{1j}^j$$

It is now clear that the L2 equation range, clock and tropospheric terms are scaled version of the L1 equation with scale factor k_2 / k_1. Likewise, the L2 ionospheric terms are scaled version of the L1 equation with scale factor k_1 / k_2. It follows that the ionosphere-free combination will be $\varphi_1^{ij} - (k_2 / k_1) \varphi_2^{ij}$ and the geometry free combination will be $\varphi_1^{ij} - (k_1 / k_2) \varphi_2^{ij}$. These combinations give the following expressions for tropospheric delay and ionospheric advance,

$$k_1^i T^i - k_1^j T^j = \frac{k_1^2}{k_1^2 - k_2^2} \left\{ \varphi_1^{ij} - \frac{k_2}{k_1} \varphi_2^{ij} - (N_1^{ij} - \frac{k_2}{k_1} N_2^{ij}) \right\} - \left(k_1^i r^i - k_1^j r^j\right) - \left(k_1^i - k_1^j\right) b$$

$$k_1^i I_{1i}^i - k_1^j I_{1j}^j = \frac{k_2^2}{k_2^2 - k_1^2} \left\{ N_1^{ij} - \frac{k_1}{k_2} N_2^{ij} - \left(\varphi_1^{ij} - \frac{k_1}{k_2} \varphi_2^{ij} \right) \right\}$$

These expression differ from the equivalent GPS equations in that the differences involve cycles of L_1^i and cycles of L_1^j and in that the ionospheric advances for satellites *i* and *j* are in meters at L_1^i and L_1^j respectively.